Supportive Information

Additive-assisted supramolecular manipulation of polymer:fullerene blend phase morphologies and its influence on photophysical processes

Ester Buchaca-Domingo,*[a] Andrew J. Ferguson,*[b] Fiona C. Jamieson,[c] Thomas McCarthy-Ward,[c] Safa Shoaee,[c] John R. Tumbleston,[d] Obadiah G. Reid,[b] Liyang Yu,[e] Marie-Beatrice Madec,[c,f] Martin Pfannmöller,[g] Felix Hermerschmidt,[a] Rasmus R. Schröder,[g,h] Scott Watkins,[i] Nikos Kopidakis,[b] Giuseppe Portale,[j] Aram Amassian,[e] Martin Heeney,[c] Harald Ade,[d] Garry Rumbles,[b,k] James R. Durrant[c] and Natalie Stingelin[a]

Received (in XXX, XXX) Xth XXXXXXXXX 20XX, Accepted Xth XXXXXXXXX 20XX

[a] *Department of Materials and Centre for Plastic Electronics, Imperial College London, London, UK; E-mail: e.buchaca-domingo@imperial.ac.uk*
[b] *Chemical and Materials Science Center, National Renewable Energy Laboratory, Golden, Colorado, USA; E-mail: andrew.ferguson@nrel.gov*
[c] *Department of Chemistry and Centre for Plastic Electronics, Imperial College London, London, UK*
[d] *Department of Physics, North Carolina State University, Raleigh, North Carolina, USA*
[e] *Division of Physical Sciences and Engineering, King Abdullah University of Science and Technology (KAUST), Thuwal, Saudi Arabia*
[f] *Solvay Interox, Warrington, UK*
[g] *CellNetworks, BioQuant, Heidelberg University, Heidelberg, Germany*
[h] *InnovationLab GmbH, Heidelberg, Germany*
[i] *Commonwealth Scientific and Industrial Research Organisation, Clayton, Australia*
[j] *ESRF Grenoble, Grenoble, France*
[k] *Department of Chemistry and Biochemistry, University of Colorado, Boulder, USA*

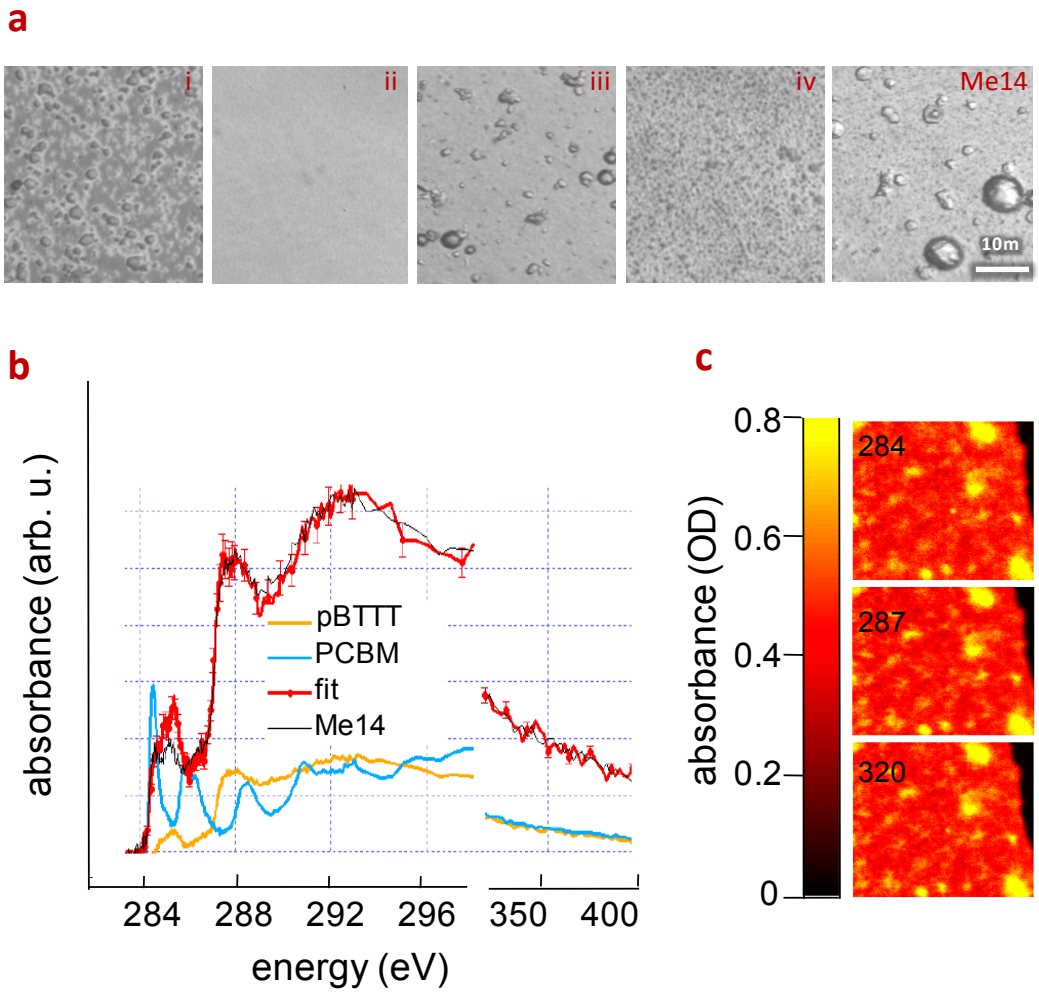

Figure S1. (a) Visible light microscope images of pBTTT (*i*), pBTTT:$PC_{61}BM$ (*ii*), pBTTT:Me12:$PC_{61}BM$ (*iii*), pBTTT:Me7:$PC_{61}BM$ (*iv*) and pBTTT:Me14:$PC_{61}BM$ (Me14). The presence of additives increases the surface roughness of the films, which exhibit large fullerene domains (verified with STXM) when long chain additives such as Me12 and Me14 are used, likely due to phase separation of the polymer and the fullerene. (b) Absorbance spectrum of pBTTT:Me14:$PC_{61}BM$ (Me14); the spectra of neat pBTTT and $PC_{61}BM$ are included for direct comparison. The absorbance spectra were employed to estimate the composition of Me14 film. We calculate a $PC_{61}BM$ content of approximately 9 wt.% supporting the picture that long additives (also seen for Me12) are able to deplete larger amounts of $PC_{61}BM$ from the mixed phase (here, the co-crystal). (c) STXM images of blends comprising Me7 using different photon energies (284, 287 and 320 eV, from top to bottom) indicating that the feature observed in pBTTT:Me7:$PC_{61}BM$ film are due to surface roughness and not $PC_{61}BM$ aggregates. Note that the absorbance images at these energies are similar however the intrinsic material mass absorptions are vastly different (as seen in Fig. S1/b). The high intensity regions are therefore not compositional heterogeneities. Instead they are thickness variations.

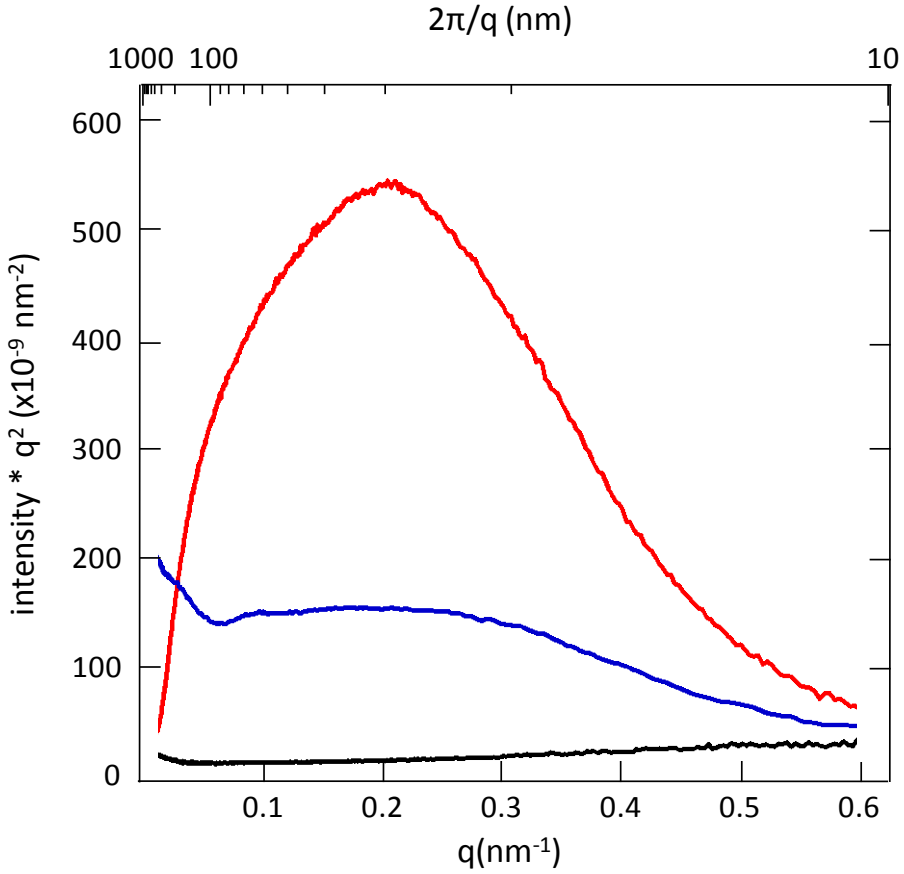

Figure S2. Lorentz corrected resonant soft X-ray scattering (R-SoXS) profiles of blend films for 284.2 eV photon energy where optical contrast between polymer and fullerene is high. There is essentially no scattering for the no additive blend (black line) over the measured length scale due to complete fullerene intercalation. Scattering is greatest for blends comprising Me7 (red line) with median characteristic length of ~25 nm. Systems with Me12 display similar features, although the scattering intensity is reduced (blue line) due to reduced composition variations over the length scales probed which is consistent with the low $PC_{61}BM$ concentration found in STXM and shown in Fig. 1c/d.

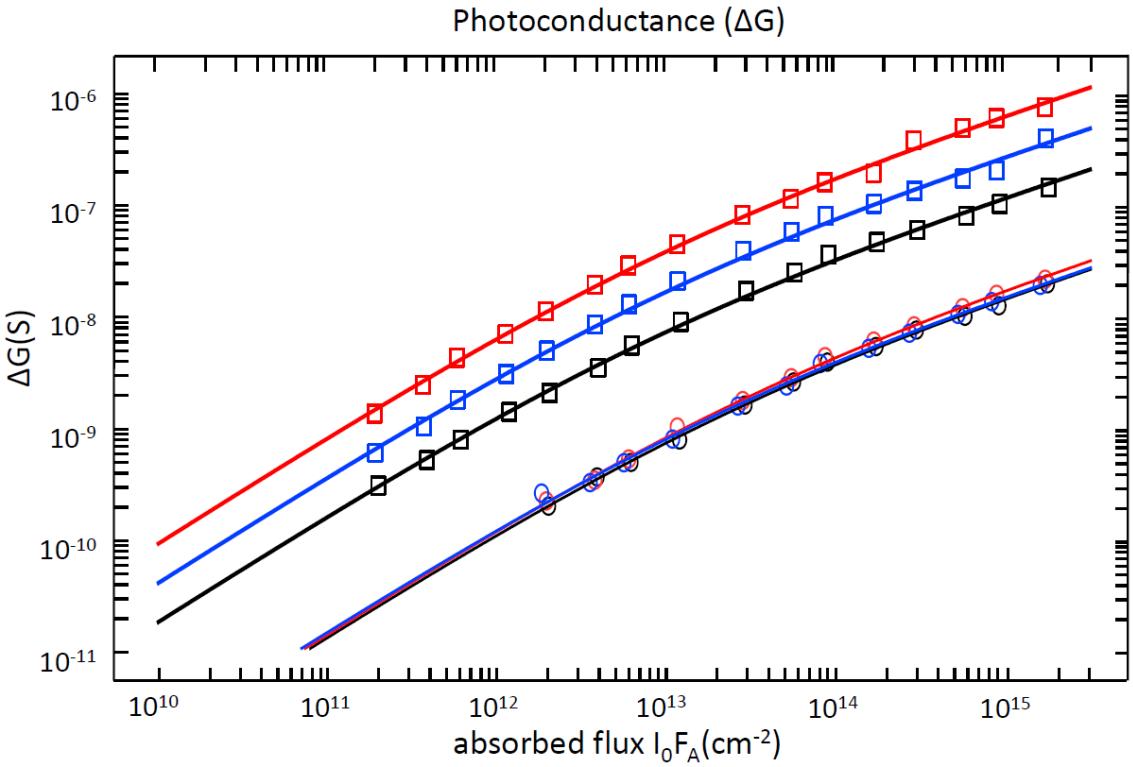

Figure S3. The product of the yield for free carrier generation per absorbed photon with the sum of the mobilities of free carriers, versus the absorbed photon flux of the pump laser pulse. The data are obtained from the peak photoconductance measured using TRMC in neat pBTTT (black circles), with additives (blue circles for pBTTT:Me12, red circles for pBTTT:Me7), the co-crystal pBTTT:$PC_{61}BM$ (black squares) and the ternary blends (blue squares for pBTTT:Me12:$PC_{61}BM$ and red squares for pBTTT:Me7:$PC_{61}BM$).

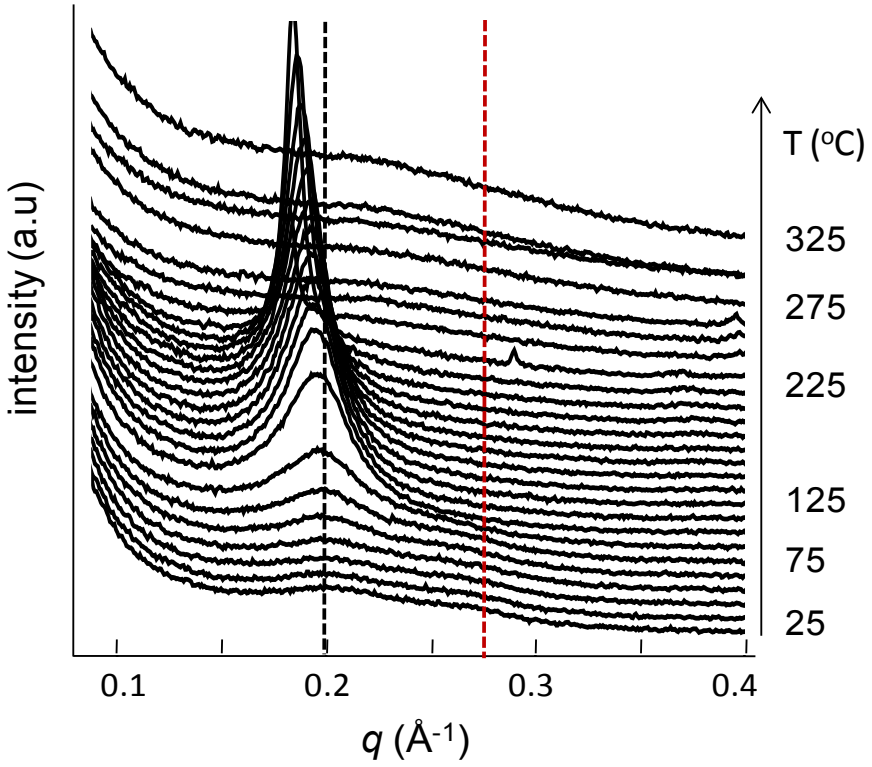

Figure S4. Temperature-dependent Wide Angle X-ray Scattering (WAXS) data of pBTTT:Me7:$PC_{61}BM$ as cast. Neat pBTTT-C16 shows d_{100} lamellar spacing close to $q \sim 0.28$ Å^{-1} indicated with a red-dash line (diffraction patterns of neat polymer and fullerene are not shown here).The black dash-line indicates the first order diffraction shifted to higher distances ($q \sim 0.2$ Å^{-1}) when the co-crystal pBTTT:$PC_{61}BM$ is formed which is more pronounced here – and even shifted to lower q values – after annealing. From these data we can deduce how higher temperatures such as 150 °C drives the fullerene intercalation and, hence, formation of 1-phase system (*i.e.* forming the co-crystal pBTTT:$PC_{61}BM$).

Table S1. Average OPV device characteristics of pBTTT:$PC_{61}BM$ (*ii*), pBTTT:Me12:$PC_{61}BM$ (*iii*) and pBTTT:Me7:$PC_{61}BM$ (*iv*). The best device performance was obtained for pBTTT:Me7:$PC_{61}BM$ (*iv*), which is comprised of 3 phases. When annealing this specific ternary (denoted here as ^{ann}*iv*) at 150 °C, which drives fullerene intercalation and, hence, formation of a 1-phase system (see Supplementary Information Figure S4), the efficiency decreases and a performance very similar to the pBTTT:$PC_{61}BM$ binary in obtained.

blends	J_{sc} (mA/cm^2)	V_{oc} (V)	*FF*	*Efficiency* (%)
pBTTT:$PC_{61}BM$ (ii)	0.55	0.39	0.27	0.06
pBTTT:Me7:$PC_{61}BM$ (iv)	2.93	0.41	0.39	0.47
pBTTT:Me12:$P_{61}CBM$ (iii)	1.09	0.39	0.32	0.14
pBTTT:Me7:$PC_{61}BM$ ann (^{ann}iv)	0.38	0.48	0.37	0.07